MECHANICAL PROPERTIES AND IMPACT TOUGHNESS OF MOLYBDENUM ALLOYED DUCTILE IRON

D. Franzen, B. Pustal, and A. Bührig-Polaczek
Foundry-Institute, RWTH Aachen University, Intzestrasse 5, 52072 Aachen, Germany

Abstract

Grades of high silicon ductile iron offer excellent combinations of static strength and ductility as well as good machinability due to their fully ferritic, solution strengthened matrix. As a result of elevated silicon contents, however, the ductile-to-brittle transition temperature in the Charpy impact test is significantly increased. Thus, minimum required Charpy impact energies cannot be met for many applications by using high silicon ductile iron. Therefore, alloys with lower strength and higher toughness properties are commonly used for many technical applications. The enormous lightweight construction potential of high silicon ductile iron can therefore not be fully exploited. The present investigation pursues the metallurgical approach of partially substituting silicon with molybdenum as an alternative strengthening element in order to improve the toughness properties while maintaining similar static mechanical properties. Molybdenum serves as a carbide-stabilising element in ductile iron,
while simultaneously promoting ferrite formation and is therefore regarded to be suitable alloying element. In Charpy impact tests, the ductile-to-brittle transition temperature could be reduced by about 55 °C by reducing the silicon content to 2.95 wt% and adding 0.21 wt% molybdenum compared to a high silicon alloy. Additionally, it was possible to mathematically describe the transition behaviour of the studied alloys using nonlinear regression functions and to achieve a sufficient correlation of empirically determined and calculated data. This present metallurgical concept offers a promising metallurgical tool for further improving the toughness properties of alloyed ductile iron.

Keywords: *cast iron, ductile iron, spheroidal graphite cast iron, silicon substitution, toughness, alloy development*

Introduction

Back in the 1950s and 60s, studies were carried out by White et al. and Peleg on ductile iron with elevated silicon contents between 4 and 5 wt%.[1,2] They found that a very good combination of strength and elongation can be achieved by solid solution strengthening of the metallic matrix. Furthermore, an increased tolerance of carbide formation due to higher silicon content was observed, which may improve the mechanical machinability of these alloys. It was in the 1990s that the idea of solid solution strengthening by alloying with silicon was taken up again by Björkegren et al., resulting in the incorporation into the Swedish Standards SS 140720 and SS 140725 and the

European Standard DIN EN 1563 in 2012.[3]-[6] In contrast to conventional strengthened grades that are characterised by a significant amount of pearlite, elevated silicon (Si) contents in the range of 3.2 to 4.3 wt% lead to the formation of a fully ferritic matrix with good machinability on the one hand, and to excellent static mechanical properties on the other. Additionally, elevated amounts of Si promote a stable eutectic solidification of carbon, resulting in higher tolerances against carbide formation, particularly in thin wall castings.[7,8] This advantageous combination of static mechanical properties and good machinability has led to a large number of casting components in a wide range of technical applications such as rotor hubs and other wind power components as well as various automotive applications like wheel suspensions and suspension arms made of high silicon ductile iron in the last years.[9]-[11]
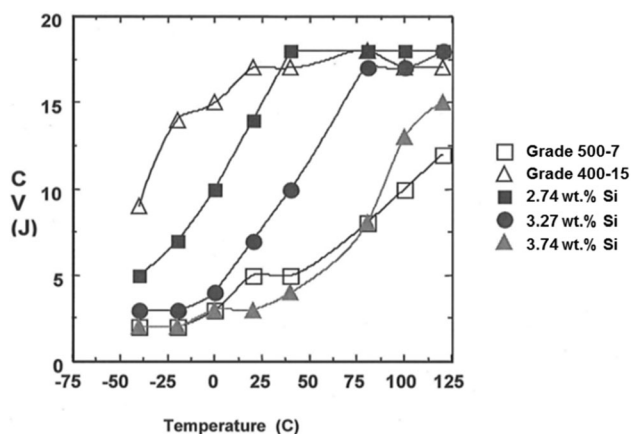
Figure 1. Variation of the impact strength with temperature for ductile irons with different Si contents, according to Björkegren and Hamberg.[6]

However, dynamic mechanical properties of high silicon ductile iron such as the Charpy impact energy can be described as significantly disadvantageous. As illustrated in Figure 1, the Charpy impact energy is rapidly reduced as the silicon content is increased. Furthermore, the ductile-to-brittle transition temperature (DBTT) is shifted to higher temperatures due to elevated silicon contents. According to studies carried out by Björkegren et al., an increase in the silicon content from 2.74 to 3.74 wt% leads to an elevation of the DBTT of about 70 °C.[6]. Because the Charpy impact test is the common testing procedure for low-temperature qualification of cast iron materials, the minimum requirements can often not be met by using high silicon ductile iron grades. In these cases, an individual qualification of these materials is carried out on the basis of fracture mechanical strength certificates as described in the FKM guideline.[12,13] For both foundrymen and designers, the aspects mentioned lead to an increased uncertainty regarding the use of castings made of high silicon ductile iron in dynamically loaded components.

It is commonly known that elevated silicon contents lead to a significant strengthening of the α-solid solution. Due to alloying with Si, iron atoms in the crystal lattice are substituted by Si atoms, resulting in a distortion of the lattice. As a result, dislocation movement during deformation is hindered and higher stresses are needed to initiate dislocation movement through the crystal lattice.[14] Due to hindering of the dislocation movement, the ductility of ductile iron materials decreases with increasing silicon contents. Studies carried out by Löblich et al. have shown that the elongation at fracture rapidly decreases to values near to zero, if the silicon content is set to 4.3 wt% a higher.[15] Weiß et al. showed that this embrittlement phenomenon is attributed to the formation of iron-silicon (FeSi) long-range orderings which appear as B2 and DO₃-ordered formations.[16] The formation of FeSi long-range ordered domains is also known from high silicon steels with up to 6.5 wt% Si that are commonly used for

electrical engineering applications such as transformers and generators.[17]

Additional numerous studies have been carried out to investigate the influence of various alloying elements on the development of mechanical properties, in particular the toughness properties. A good summary of the single effects of different alloying elements is given in.[18] In ferritic ductile iron, nickel leads to an increase in tensile strength of 30 MPa per wt%, while the DBTT increases only slightly compared to the addition of silicon.[19] For this reason, in many applications, a partial substitution of silicon by nickel as an alternative strengthening element is applied.[20]

The impact energy of ductile iron materials is considerably affected by the pearlite content. Studies carried out by Sandoz et al. demonstrate that an increase in the pearlite content from 10 to 75% lead to a shift of the DBTT in the Charpy V-notch impact test from about 10 to 50 °C. Additionally, the upper shelf energy (USE) is lowered from about 18 to 15 J.[21] The effect of the pearlite content on the Charpy impact energy is confirmed by studies from Hafiz et al. and Toktas et al.[22,23]

In order to reduce the negative effect of silicon on the Charpy impact strength in ductile iron, previous studies aimed at partially substituting silicon by alternative solid solution-strengthening elements such as nickel and aluminium. Based on material grade SGI 500-14, Weiß et al. achieved similar strengths as in SGI 500-14 by substituting up 0.8 wt% Si with both 1.1 and 1.5 wt% Ni in combination with 0.2 wt% Al and was able to increase the Charpy impact energy in the temperature range of 20 °C and about 60 °C by about 2–3 J.[24]

Investigations on the effect of molybdenum (Mo) as a carbide-promoting element on the mechanical properties of ductile iron have been carried out by Hernandez-Avila et al.[25] They showed that the ultimate tensile strength (UTS) increases from 579 to 647 MPa due to the addition of 0.38 wt% Mo. At the same time, the elongation at fracture (A) is decreased from 15 to about 10%. The authors state that the DBTT in the Charpy impact energy is increased by about 39 °C as the Mo content is raised by 1 wt%. Furthermore, it is assumed by the authors that Mo is dissolved in the ferrite matrix, serving as a solid solution-strengthening element. However, according to Hasse, Mo segregates positively, accumulating in last-to-freeze areas and resulting in promotion of carbide formation during eutectic solidification.[26] Furthermore, ferrite formation is promoted in ductile iron, when alloyed with Mo in contents of 0.1–0.3 wt%.[18] It is assumed that higher contents of Mo even favour the formation of bainite and martensite. Mo serves as a common alloying element for ductile iron and is widely used for the production of SiMo cast iron materials. While silicon acts as a ferrite-stabilising due to an increase in the eutectoid transformation temperature and leads to the formation of an oxidation-

Table 1. Chemical Compositions of the Investigated Alloys (Contents in wt%, Carbon Content Determined via Thermal Analysis)

Alloy	C	Si	Mn	P	S	Mo	Ni	Mg	CE
1	3.69	2.10 ± 0.03	0.09 ± 0.002	0.001 ± 0.001	0.006 ± 0.001	0.002 ± 0.001	0.18 ± 0.003	0.044 ± 0.003	4.41
2	3.19	3.03 ± 0.02	0.18 ± 0.003	0.001 ± 0.001	0.001 ± 0.001	0.004 ± 0.001	0.03 ± 0.003	0.039 ± 0.004	4.20
3	2.96	3.64 ± 0.07	0.15 ± 0.003	0.001 ± 0.001	0.001 ± 0.001	0.003 ± 0.001	0.02 ± 0.002	0.040 ± 0.004	4.18
4	3.47	2.95 ± 0.09	0.13 ± 0.01	0.015 ± 0.002	0.006 ± 0.001	0.21 ± 0.005	0.024 ± 0.005	0.0354 ± 0.003	4.46

resistant surface layer, Mo increases high-temperature strength of these materials, which allows them to be used at elevated temperatures of up to 860 °C.[27,28]

Based on these results, it is assumed that partial substitution of silicon can serve as a suitable metallurgical tool in order to reduce the negative effect of silicon on the Charpy impact energy and to improve the DBTT in technical relevant ranges while maintaining similar static mechanical properties.

In the present study, molybdenum is chosen as an alternative strengthening alloying element in ductile iron. This metallurgical approach is based on both the ferrite-stabilising and carbide-promoting effect in ductile iron materials and aims at partially substituting Si with Mo. The alloy modified in this way is compared to conventional ductile iron grades with varying Si contents and analysed regarding their microstructure and mechanical properties.

Design of Experiments

In order to determine the substitutional effect of molybdenum on the mechanical properties of high silicon DI, four different casting series were produced and analysed regarding their microstructure and their static and dynamic mechanical properties in terms of impact toughness. These series are referred to as alloy 1–4. As Table 1 shows, alloy 1 is based on grade SGI 400-18 and contains 2.1 wt% Si and 0.18 wt% nickel (Ni). In alloy 2 and 3, the silicon content is increased to 3.0 wt% and 3.64 wt%, respectively. Therefore, alloy 3 is based on grade SGI 500-14. Alloy 4 was studied in order to partially substitute silicon. Compared to alloy 3, the Si content was reduced by 0.69 wt% to 2.95 wt% Si. To investigate the effect of molybdenum as a potential substituting alloying element, the Mo content was set to 0.21 wt%.

Experimental Procedure

A total of 4 alloys, referred to as alloy 1–4, was produced and examined, mainly differing in silicon content (2.10–3.64 wt%) and molybdenum content (0–0.2 wt%). While alloys 1–3 primarily show differences in the silicon content, the silicon content in alloy 4 was intentionally reduced and a molybdenum content of 0.2 wt% was alloyed simultaneously. The final chemical composition of the alloys is given in Table 1. All alloys were set to a near-eutectic composition with a carbon equivalent (CE) of 4.28, calculated according to Eqn. 1.

$$CE = \%C + \frac{1}{3}(\%Si + \%P) \qquad \text{Eqn. 1}$$

For producing of the alloys, raw materials consisting of recirculation material (grade SGI 400-15), high purity iron

and ferrosilicon (FeSi75) were prepared and melted in a 250 kg medium-frequency induction. For alloy 4 containing 0.2 wt% Mo, pre-alloy FeMo65 was charged into the furnace, additionally. After melting, the melt was overheated to 1500 °C and held for 5 min in order to remove impurities from the melt. After deslagging and casting samples for spectrometric analysis, the magnesium treatment with 1.3 wt% of a cerium-free magnesium master alloy and a grain size of 4–10 mm at 1430 °C was performed by using the sandwich method. Therefore, 1.4 wt% of a cerium-free magnesium pre-alloy (45 wt% Si, 6.25 wt% Mg, 1.9 wt% Ca) and 0.3 wt% of a cerium-containing inoculant (64–70 wt% Si, max. 1.2 wt% Al, 1.8–2.4 wt% Ca, 0.8–1.2 wt% Bi, 0.8–1.2 wt% Ce) with a grain size of 0.6–2 mm were placed onto the bottom of a pouring ladle and were covered with 4 wt% of low-alloyed steel scrap. After the magnesium treatment, the melt was deslagged. Shortly before casting, samples for both thermal analysis and spectrometric analysis were produced, and the melt was cast at about 1350 °C. The pouring temperature was measured manually shortly before pouring. For each alloy, two furan-bonded sand moulds, each containing Y-shaped test blocks according to EN 1563 (2 Y_{II} and 2 Y_{IV} standard test blocks per mould with wall thicknesses of 25 mm and 75 mm, respectively), were produced, as shown in Figure 2.

Per alloy a total of 2 tensile test specimen, 2 metallographic specimens and up to 25 Charpy V-notch specimens were machined out of Y_{II} test blocks. Additionally, 4 tensile test specimen according to positions a and c and 3 metallographic specimen were produced out of Y_{IV} standard test blocks.

Samples for spectrometric examinations were produced by pouring the melt in a copper die directly after inoculation and prior to casting. They were then ground with grinding paper (80-SiC) and tested using a spark emission spectrometer.
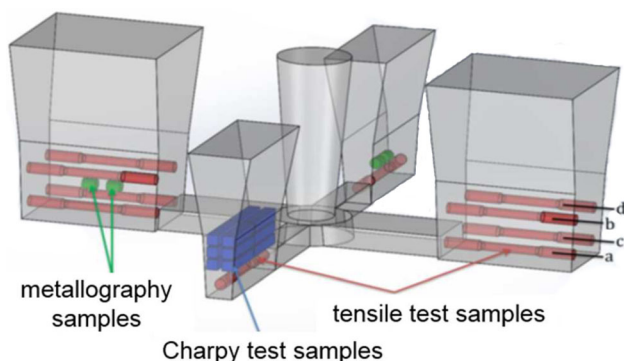

Figure 2. Casting geometry and position of samples for metallographic and mechanical analysis.

Specimen Analyses

For quasi-static tensile tests, cylindrical samples with a diameter of 18 mm were taken from the standard test blocks using a water-cooled core drill. Tensile test specimens of shape A according to DIN EN 50125 were machined with a testing diameter of $d_0 = 8$ mm and an overall length of 115 mm .[29] After machining of the specimens, tensile tests were conducted using a main cross speed of 0.60 mm/min.

For each alloy, 18–24 Charpy V-notch specimens were machined from two Y_{II} standard test blocks. The samples were then tested on a *Zwick/Roell HIT50P* pendulum impact tester with a maximum impact energy of 50 J in the temperature range of − 60–120 °C, conducting three measurements per temperature, according to DIN EN ISO 148-1.[30]

Metallographic samples were taken from the direct vicinity of the tensile and Charpy test specimens. After cold-embedding and grinding (180, 320, 500 and 1000 SiC grinding paper), metallographic samples were polished (9, 3 and 0.25 μm) using a diamond suspension. Microstructural analyses of both polished and nital-etched (0.3% HNO_3) specimens were carried out using an optical up-light microscope and automated image analysis. Per specimen a total of five images was taken and analysed regarding the nodularity, the nodule count and the pearlite fraction by converting the images into binarised micrographs. In agreement with ISO 945-4, the nodularity and the nodule count were then determined according to Eqns. 2 and 3.[31]

$$p_{Nod} = \frac{A_{VI} + A_V}{A_{all}} \qquad \text{Eqn. 2}$$

$$\text{Nod.Count} = n_V + n_{VI} \qquad \text{Eqn. 3}$$

For visualising the microsegregation behaviour of molybdenum, etchings according to Klemm[32] were carried out on single samples of alloy 4.

After solidification, samples for spectrometric analysis were prepared by grinding with 80 SiC paper. For each sample, at least three measurements were performed on a *Hitachi model OE750* spectrometer.

Results

Microstructural Analysis

Table 2 shows the summary of the results from the automated image analysis. As it can be seen, the nodularity calculated according to ISO 945-4 tends to decrease with increasing Si content. The negative influence of Si on the formation of the graphite phase, especially on the nodularity, is in agreement with the literature. In contrast, the

Alloy	Nodularity (%)		Nodule count (1/mm^2)		Pearlite content (%)	
	Y_{II}	Y_{IV}	Y_{II}	Y_{IV}	Y_{II}	Y_{IV}
1 (2.10% Si)	86.5 ± 3.5	85.0 ± 3.4	120.7 ± 8.2	130.0 ± 17.6	41.5 ± 1.4	8.1 ± 0.9
2 (3.03% Si)	75.2 ± 4.5	76.8 ± 6.1	137.5 ± 14.3	119.9 ± 10.3	26.9 ± 3.2	11.2 ± 1.3
3 (3.64% Si)	73.0 ± 5.1	61.1 ± 6.2	154.7 ± 12.4	140.1 ± 13.5	15.5 ± 4.2	9.6 ± 1.7
4 (2.95% Si + 0.2% Mo)	72.5 ± 5.3	74.5 ± 4.1	170.8 ± 6.9	148.6 ± 7.9	2.5 ± 1.7	2.3 ± 1.5

nodule count increases with increasing silicon content in alloy 1–3. However, alloy 4 shows the highest nodule count at 170.8 1/mm^2 despite a Si content of only 3.0 wt%. This tendency can also be observed in samples of Y_{IV} wedges. While Hernandez-Silva et al. cannot detect an influence of Mo on the nodule count in ductile iron,[25] investigations by Riebisch et al. show that the nodule count in Y_{II} test block samples slightly increases as the Mo content is increased from 0 to 0.27 wt%.[33] Additionally, the highest CE of 4.46 obtained in alloy 4 could increase the nodule count.

In accordance with the literature, the pearlite content decreases, as the silicon content is increased, since the ferritising potential is elevated by the addition of silicon. Additionally, higher nodule counts and therefore shorter carbon diffusion paths favour the formation of pearlite during eutectoid transformation. As a results, the highest pearlite content of 41.5% is observed in alloy 1. According to Hasse, molybdenum in contents of 0.1–0.3 wt% has a ferritising effect during the eutectoid transformation.[18] This is confirmed by the significantly reduced pearlite content in Y_{II} and Y_{IV} samples of alloy 4 compared to alloys 1–3. It is assumed that the higher nodule count in alloy 4 also has an impact on the reduced pearlite formation. As the nodule count is raised, diffusion paths for

carbon atoms during and after eutectic solidification are reduced, leading to a promotion of ferrite formation.

In order to study the segregation behaviour of molybdenum on a qualitative basis, Klemm's etchings have been carried out on samples of alloy 4. As shown in Figure 3, Mo carbides can be detected in last-to-freeze areas indicating positive segregation behaviour of molybdenum. Conducting Klemm's etchings on overall three samples of alloy 4 and subsequent line sectioning method resulted in an average carbide content of 0.2 ± 0.04%.

Mechanical Properties

The results of the static mechanical properties of the investigated alloys are shown in Table 3. Minimum values for UTS and YS of 442 MPa and 261 MPa, respectively, can be observed in Y_{II} samples for alloy 1 with the lowest Si content of 2.10 wt%. This is due to the lowest Si content of 2.10 wt%, which leads to a weak strengthening of the ferrite solid solution compared to alloys 2 and 3. Moreover, the comparatively highest nodularity of 86.5% ensures low stress concentrations in the matrix during loading, which in addition leads to increased ductility. The average UTS of 442 MPa corresponds to the required minimum specifications for wall thicknesses below 30 mm according to EN 1563 for material grade SGI 400-18.[5] Simultaneously, the highest elongation at fracture (A) is achieved in Y_{IV} samples, which is attributed to a significant lower pearlite content compared to Y_{II} samples due to reduced cooling rates.

When the Si content is increased, both UTS and YS in Y_{II} samples increase considerably, which is due to the additional effect of ferrite solid solution strengthening by Si. In Y_{II} samples of alloy 3, a UTS of 522 MPa and an elongation at fracture of 21.3% is obtained, which corresponds to the minimum requirements of grade 500-14 according to EN 1563. As the Si content increases, the ratio YS/UTS increases clearly, as commonly known from the current state-of-the-art.[5] Thus, the capacity for plastic deformation of the material decreases significantly. This is confirmed in particular by a decrease in the uniform strain A_g in from 16.5% to 13.9% in alloy 3. In alloy 4, a UTS of 470 MPa is
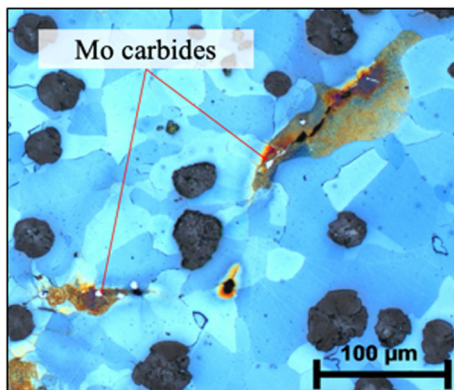

Figure 3. Klemm's etching of a Y_{II} sample of alloy 4 at 100 × magnification, visualising Mo carbides in last-to-freeze areas.

Table 3. Static Mechanical Properties of Alloys 1–4

Alloy	UTS (R_m)		YS ($R_{p0.2}$)		A (Elong. %)		Ag (Uniform strain %)		YS/UTS	
	Y_{II}	Y_{IV}	Y_{II}	Y_{IV}	Y_{II}	Y_{IV}	Y_{II}	Y_{IV}	Y_{II}	Y_{IV}
Alloy 1 - 2.10% Si + 0.18% Ni	442 ± 6	391 ± 4	261 ± 3	237 ± 1	20.6 ± 2.0	28.6 ± 0.6	16.5 ± 1.0	18.5 ± 0.1	0.59	0.61
Alloy 2 - 3.03% Si	484 ± 4	470 ± 1	336 ± 1	328 ± 1	21.7 ± 1.2	24.9 ± 1.1	16.2 ± 2.2	16.1 ± 0.1	0.69	0.70
Alloy 3 - 3.64% Si	522 ± 1	551 ± 2	399 ± 0	419 ± 2	21.3 ± 1.2	20.6 ± 1.4	13.9 ± 0.2	13.7 ± 0.3	0.76	0.76
Alloy 4 - 2.95% Si + 0.21% Mo	470 ± 3	463 ± 3	333 ± 1	326 ± 1	23.4 ± 0.6	22.5 ± 0.7	15.7 ± 0.7	15.5 ± 0.2	0.71	0.70

obtained in Y_{II} samples, while the YS amounts to 333 MPa. Thus, the requirements of EN 1563 for grade 500-14 cannot be fully met, which is assumed to be due to a slightly lower Si content in alloy 4 compared to alloy 2. According to Riebisch et al., the impact of Mo on the UTS and YS of high silicon ductile iron can be regarded as minor.[34] With an average elongation at fracture of 23.4% and a uniform strain of 15.7%, slightly higher ductility was achieved compared to alloy 2. Although the increase in elongation at fracture of alloy 4 is only minor, this tendency could be attributed to the reduction in the Si content and to the effect of molybdenum addition: Firstly, molybdenum seems to promote ferrite formation, as stated by Hasse.[18] Additionally, a higher nodule count is observed in alloy 4 leading to an increase in ductility. A summary of the static mechanical properties obtained from Y_{II} samples is given in Figure 4.

As shown by Björkegren et al., the transition temperature DBTT is shifted to higher temperatures with increasing silicon content,[6] which is also observed in the present study. Additionally, the transition range between ductile and cleavage fracture behaviour is extended due to an increase in silicon. As suggested in the standard EN ISO 148-1 and stated in the technical specification SEP 1670, the DBTT was defined by determining the temperature at half of the upper shelf energy (USE).[30,35] As indicated in Figure 5, the DBTT in alloy 1 is about − 22 °C and is shifted to 19 and 65 °C, respectively, due to the increased Si content in alloy 2 and 3. It can therefore be calculated that the DBTT is increased by about 43.5 °C due to the addition of 1 wt% Si.

By reducing the Si content to 2.95 wt% and adding 0.2 wt% Mo in alloy 4, the DBTT is reduced by almost 60–7 °C compared to alloy 3. Additionally, the DBTT is 13 °C lower than that of alloy 2, which is attributed to both a higher nodule count and lower pearlite contents. Literature data shows that an increase in the nodule count in ferritic DI leads to a significant reduction in the DBTT.[36] Furthermore, lower pearlite contents in alloy 4 according to[21] also lead to a shift of the DBTT to lower temperatures.

While upper shelf behaviour and complete ductile fracture can be expected from temperatures above 80 °C in alloy 3, complete ductile failure in alloy 4 is already observed at 40 °C. Additionally, due to the almost fully ferritic matrix, the USE increases to 14 J, which is confirmed by the literature. Higher USE in alloy 4 results in higher energy absorption during impact loading while simultaneously providing higher UTS and YS compared to alloys 2 and 3.

According to the technical specification SEP 1670 that was particularly developed for the characterisation of the Charpy impact toughness of forged steels in 2010 ,[35] the transition curve determined by Charpy impact tests can mathematically be described using a tanh function, as indicated in Eqn. 4. Here, E_L is the lower shelf energy, E_U is the upper shelf energy, a and T_x are fitting parameters and d is a asymmetry parameter:

$$A_v(T) = E_L + (E_U - E_L) \times \left[\frac{1 + \tanh(a \times (T - T_x))}{2} \right]^d$$

Eqn. 4

This nonlinear regression function was applied to ductile iron alloys 1–4. In order to fit the regression function to the experimental results, d was constantly set to 1.9 for all investigated alloys, and E_L and E_U were determined based on the Charpy impact tests conducted. Subsequently, a nonlinear regression analysis was performed. Therefore, the fitting parameters a and T_x were varied and the fitting curve was calculated using the least error square method. Figure 6 shows the regression analysis and the correlation degree R^2. Based on the results of the impact tests, it can be observed that there is a very good correlation of measured and calculated Charpy impact toughness for all of the investigated alloys. However, the degree of correlation for the description of the transition behaviour in alloy 3 is slightly lower. This is attributed to both the presence of two transition ranges (at approx. 0–20 °C and 60–80 °C) and the widening of the transition range due to the increased Si content of 3.64 wt%. A similar observation can be made on the basis of measurements by Björkegren et al.[6] A summary of the final regression functions for alloys 1–4 is given in Eqs. 5–8.
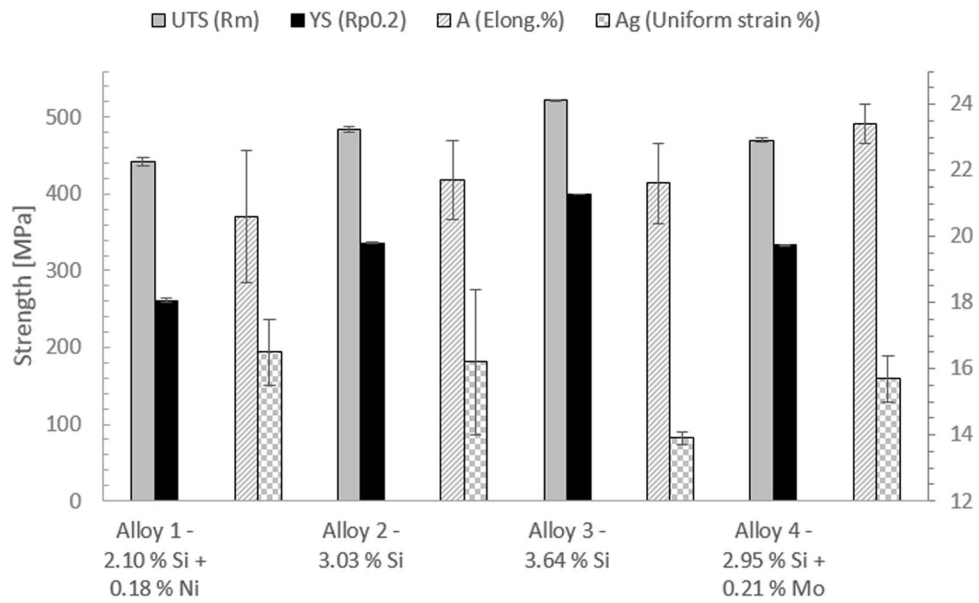
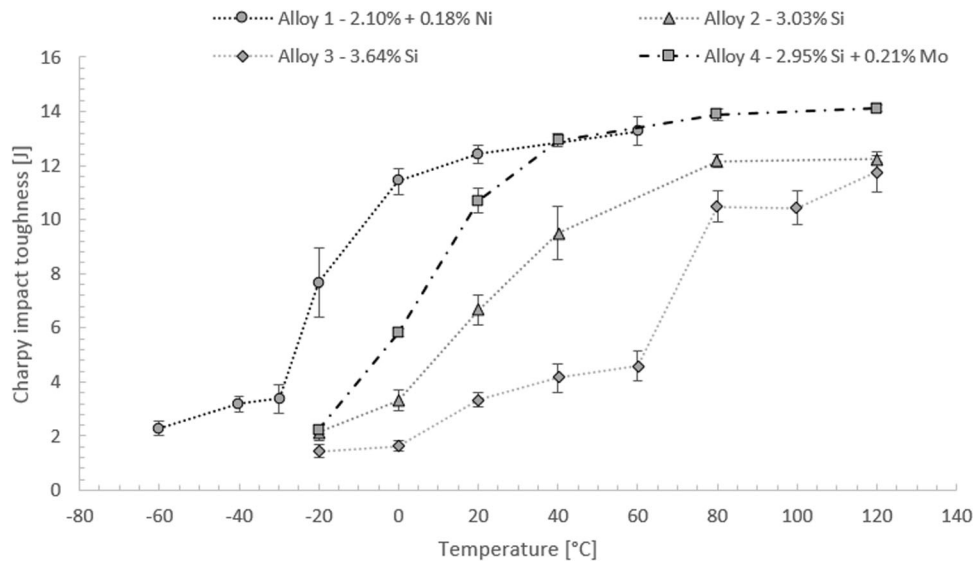**Figure 4.** *Static mechanical properties of the investigated alloys obtained from Y_{II} samples.*

Figure 5. *Charpy V-notch impact energy obtained from Y_{II} samples of alloys 1–4.*
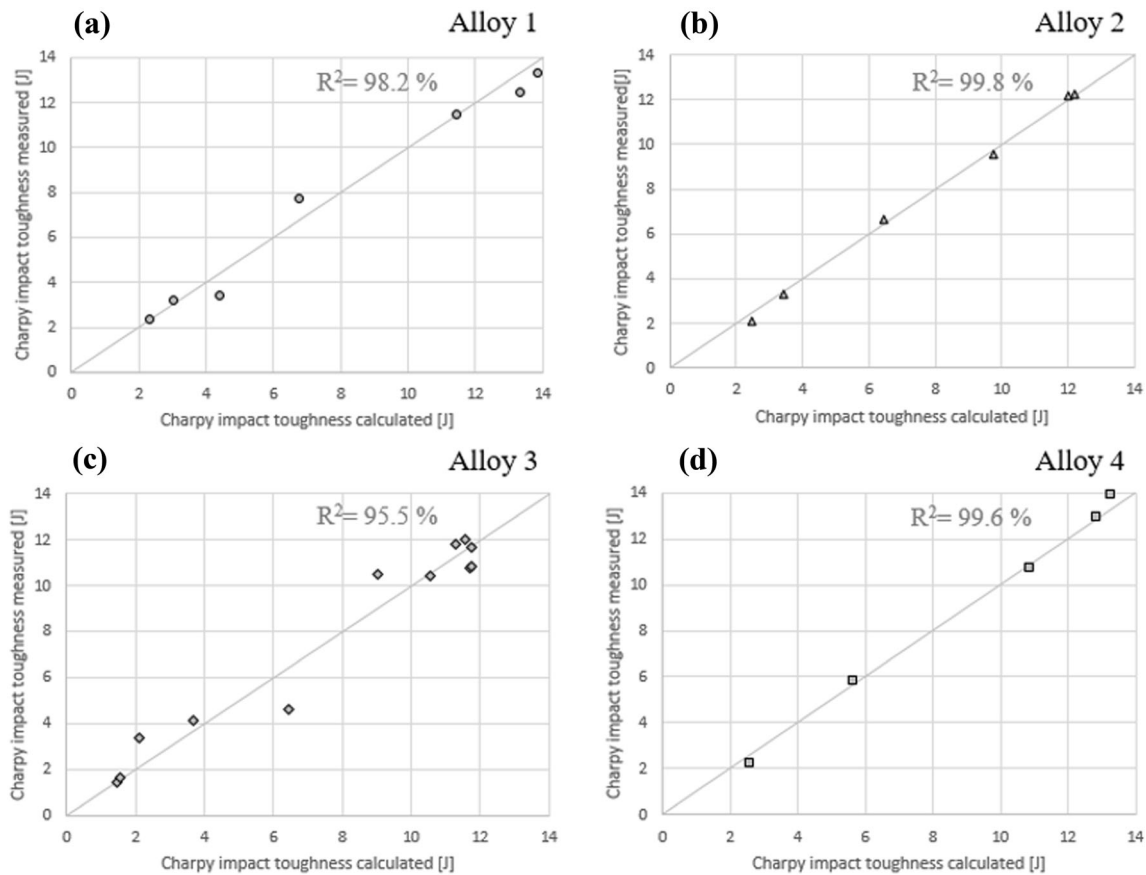
Figure 6. Correlation of the calculated and measured Charpy impact energy for all investigated alloys; (a) alloy 1 (2.10 wt% Si), (b) alloy 2 (3.03 wt% Si), (c) alloy 3 (3.64 wt% Si), (d) alloy 4 (2.95 wt% Si + 0.21 wt% Mo).

Alloy 1

$$A_v(T) = 2.3 + (13.9 - 2.3)$$
$$\times \left[\frac{1 + \tanh(0.040 \times (T - 25.42))}{2} \right]^{1.9}$$

Eqn. 5

Alloy 2

$$A_v(T) = 2.3 + (12.2 - 2.3)$$
$$\times \left[\frac{1 + \tanh(0.032 \times (T - 11.75))}{2} \right]^{1.9}$$

Eqn. 6

Alloy 3

$$A_v(T) = 1.4 + (11.8 - 1.4)$$
$$\times \left[\frac{1 + \tanh(0.024 \times (T - 44.2))}{2} \right]^{1.9}$$

Eqn. 7

Alloy 4

$$A_v(T) = 2.2 + (14.1 - 2.2)$$
$$\times \left[\frac{1 + \tanh(0.045 \times (T - 1.61))}{2} \right]^{1.9}$$

Eqn. 8

Fracture Surface Analysis

Figure 7 shows the fracture surfaces of Charpy specimens tested in Charpy impact tests at room temperature (RT). It can be seen that alloy 1 shows completely ductile fracture at this temperature due to the lowest Si content of 2.10 wt%. Alloy 3 with a Si content of 3.03 wt% shows almost complete cleavage fracture at RT at an impact energy of approx. 6.6 J. Correspondingly, alloy 3 alloyed with 3.64 wt% Si exhibits complete cleavage fracture at this temperature. Alloy 4 exhibits an impact energy of approx. 10.7 J at RT and is characterised by a mixed fracture with a predominant proportion of ductile fracture.

Discussion

Based on the results of the microstructural analysis, it was observed that silicon has a significant influence on the formation of the graphite phase. While the nodularity decreases with increasing Si content, an increase in the nodule count is studied. By alloying with 0.21 wt% Mo, the pearlite content in alloy 4 can be significantly reduced, confirming the ferrite-stabilising effect of molybdenum.[18] Furthermore, a tendency could be observed that the nodule
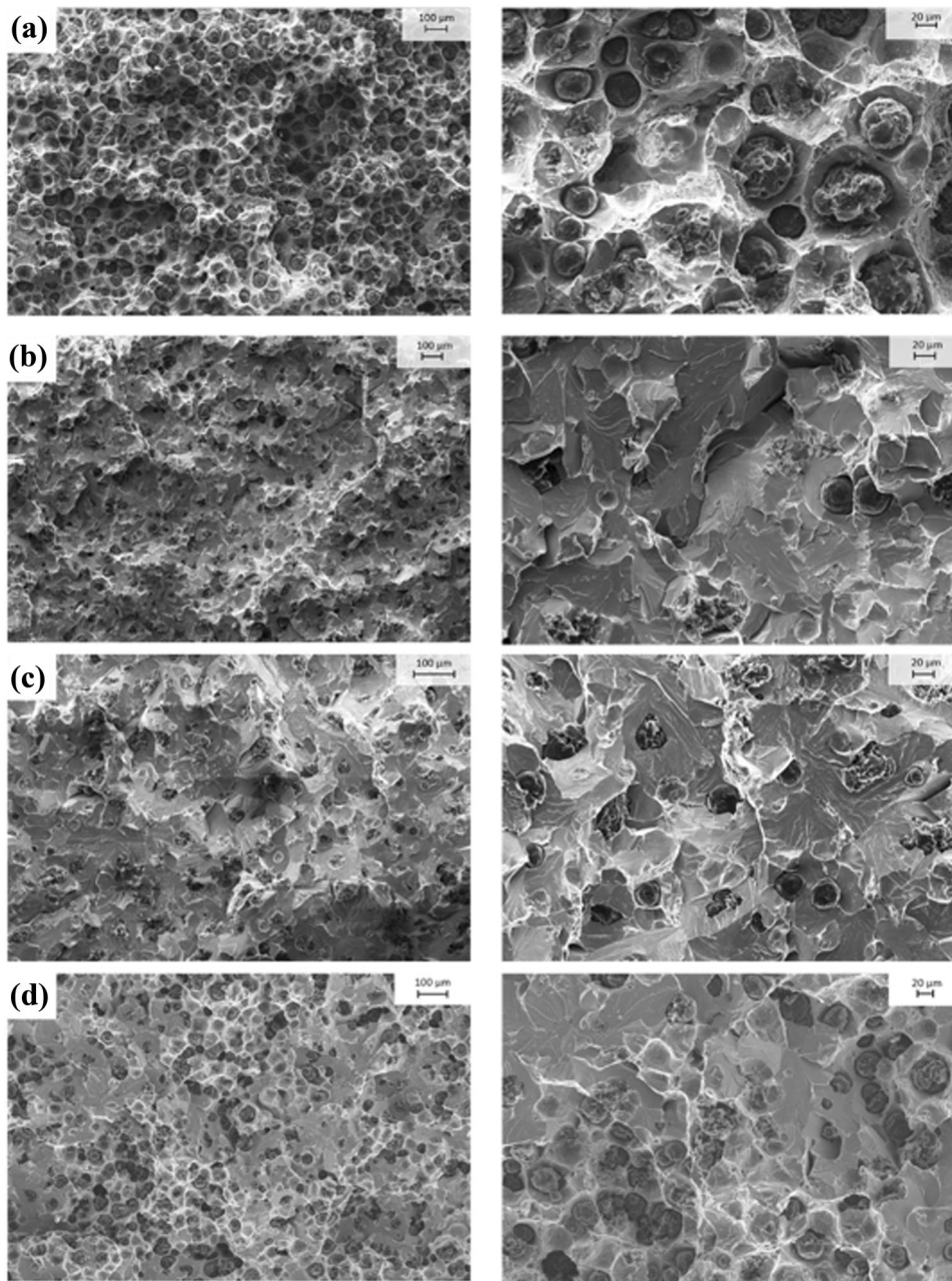
Figure 7. Fracture surface analysis of the investigated alloys 1–4 via SEM at RT; (a) 2.10 wt% Si, (b) 3.03 wt% Si, (c) 3.64 wt% Si, (d) 2.95 wt% Si + 0.21 wt% Mo at 200 × and 500 × magnification.

count increases slightly as a result of the addition of Mo. However, this increase cannot be considered as statistically significant due to the high variability in the values for the nodule count. The results of Klemm's etchings confirmed that molybdenum acts as a carbide-stabilising alloying element and leads to carbide formation in last-to-freeze areas.

The influence of carbide formation on the strength in alloy 4 is considered to be low, as slightly lower values for UTS are achieved compared to alloy 2. In addition to the pearlite content, the mechanical properties of the

investigated alloys are significantly influenced by the Si content. However, minimum values for UTS and YS based on EN 1563 for grades SGI 500-14 cannot be met in alloy 4. This is attributed primarily to a relatively low Si content. However, minimum required values according to the specifications for elongation are fulfilled. The results of Hernandez-Silva with regard to the significant increase in strength by Mo can therefore not be confirmed.[25] Based on the present results, the Mo content could be further increased while maintaining the same Si content in order to set sufficient values for UTS and YS. To avoid formation of cementite and a coupled reduction in elongation at

fracture, the carbide content in Y_{II} wedges should be limited to about 1.5 wt%—therefore, a Mo content of about 0.4 wt% can be recommended. Since the price for the alloying element Mo is comparatively high, the simultaneous adjustment of the Si content to moderate contents of about 3.1 wt% offers an alternative possibility to achieve sufficient static and dynamic mechanical properties.

With regard to Charpy impact energy, Si is as well regarded to be the main factor influencing the transition behaviour of ductile iron. Based on the results, the transition temperature DBTT in Y_{II} standard test blocks is raised by an average of 43.5 °C by adding 1 wt% Si. However, compared to studies conducted by Björkegren et al., a smaller effect on the increase in DBTT is determined.[6] The significant reduction in the DBTT of alloy 4 is due to the reduction in the Si content from 3.64 to 2.95 wt% and the associated lower pearlite content on the one hand and to the increased nodule count on the other, which is confirmed by the literature data for ductile iron.[36] At the same time, the addition of Mo leads to an increase in the USE, which is at the same level as for alloy 1 with 2.10 wt% Si.

By means of nonlinear regression, it could be shown that the regression equation shown in Eqn. 4 can be transferred and applied to ductile iron materials in order to describe their transition behaviour in the Charpy impact test. Furthermore, a very good correlation with at least $R^2 = 95\%$ between measured and calculated Charpy impact energy could be determined.

The results of the present investigation show that alloy development concepts based on the partial substitution of Si by alternative alloying elements can be successfully applied, in particular to optimise the toughness properties of ductile iron. As seen in,[24] alternative solid solution-strengthening elements such as Ni, but also potentially carbide-stabilising elements such as Mo, showing an additional ferrite-stabilising effect, can be used for this purpose. In contrast to negatively segregating elements such as silicon, positively segregating elements such as molybdenum cause a complementary strengthening in last-to-freeze areas leading to an improved fracture behaviour. Further investigations on the influence of carbide-stabilising elements can reveal that the DBTT of cast iron alloys can be improved with adapted alloy design. Corresponding material concepts should aim at reducing the Si content on the one hand and the pearlite content on the other. Furthermore, on the basis of the current results, it is recommended to set elevated nodule counts that could be achieved by a two-step inoculation in order to further promote ferrite formation leading to a reduction in the DBTT.

Conclusions

The aim of the present investigation was the partial substitution of silicon by alternative strengthening elements based on the alloy SGI 500-14. Due to its good static mechanical properties, this alloy is ideally suited for lightweight construction applications. However, the comparatively lower impact energy and high transition temperatures due to the increased Si content prevent a broad application of these materials. In the present study, the capability of molybdenum as a potential substitutional alloying element in ductile iron was carried out. Microstructural characteristics as well as static and dynamic mechanical properties were studied based on alloys with varying Si and Mo content. The transition behaviour of the alloys investigated was mathematically described using nonlinear regression functions. The results based on the studies can be summarised as follows:

1. Molybdenum acts as a carbide-stabilising element, promoting the formation of carbides in last-to-freeze areas. An addition of 0.21 wt% Mo results in an average carbide fraction of 0.2% in Y_{II} samples.
2. The static mechanical properties of ductile iron are mainly influenced by the silicon content. It is assumed that a combined reduction in the silicon content and alloying with alternative strengthening and ferrite-stabilising alloying elements such as Mo can lead to fully ferritic alloys, resulting in excellent combinations of static mechanical properties that fulfil the requirements according to the standard EN 1563.
3. By reducing the Si content to 2.95 wt% and a combined alloying with 0.21 wt % Mo, it was possible to shift the transition temperature DBTT from about 60 °C to 6 °C. As a result, predominant ductile fracture behaviour could be observed at typical application temperatures of 20 °C. Due to improved toughness properties combined with very good static mechanical properties, the high application and lightweight construction potential of ductile iron with elevated Si contents can be further exploited.
4. It was shown that the transition behaviour of ductile iron materials can successfully be described using nonlinear regression based on a tanh function that was originally developed for forged steel alloys. In the present analysis, a degree of correlation of at least 95% is achieved for alloy 1–4. By applying the regression equation shown here, it is possible to calculate temperature-dependent minimum values for the Charpy impact energy, if required. The minimum Charpy impact energy is derived from the

calculated $A_v(T)$ curve for the corresponding temperature.

5. Molybdenum can act as a substitutional alloying element in ductile iron in order to improve Charpy impact energy while maintaining similar static mechanical properties. Alloying concepts should therefore aim at a simultaneous reduction in the Si content and the addition of alternative strengthening alloying elements like Mo.

Compliance with Ethical Standards

Conflict of interest The authors declare that they have no conflict of interest.

REFERENCES

1. W. H. White, L. P. Rice, A. R. Elsea. *Influence of Silicon Content on Mechnical and High-Temprature Properties of Nodular Cast Iron*. AFS Transactions, pp. 337–345 (1951)
2. J. Peleg. The british foundryman, 57, 436 ff (1964)
3. Swedish Standard Institute—Materialteknik. *SS140720—Spheroidal graphite cast iron.* (1998)
4. Swedish Standard Institute—Materialteknik. *SS140725—Spheroidal graphite cast iron.* (1998)
5. Deutsches Institut Für Normung E.V. *DIN EN 1563: Gießereiwesen—Gusseisen mit Kugelgraphit.* (2012)
6. L.-E. Björkegren, K. Hamberg. Silicon alloyed ductile iron with excellent ductility and machinability. In *Proceedings of the Keith Millis Symposium on Ductile Iron*, Hilton Head Island, SC, USA, (2003)
7. J.F. Janowak, R.B. Gundlach, A modern approach to alloying gray iron. AFS Trans. **90**, 847–863 (1982)
8. M. Riebisch, B. Pustal, A. Bührig-Polaczek, Influence of carbide promoting elements on the microstructure of high silicon ductile iron. Int. J. Metalcast. (2020). https://doi.org/10.1007/s40962-020-00442-1
9. R. Larker, Solution strengthened ferritic ductile iron ISO 1083/JS/500-10 provides superior consistent properties in hydraulic rotators. China Foundry **6**(4), 343–351 (2009)
10. P. Mikoleizik, G. Geier, SiWind—werkstoffentwicklung für offshore-windenergieanlagen im multi-megawatt-bereich. Giesserei **101**(9), 64–69 (2014)
11. J. Goroncy, Neues Gusseisen wiegt Leichtbaudefizite auf. VDI Nachrichten **1**(4), 67–74 (2012)
12. T. Schmidt, Festigkeitsnachweis von Eisengussteilen nach der FKM-Richtlinie. Giesserei Rundschau **50**(7), 15–22 (2003)
13. Forschungskuratorium Maschinenbau (Fkm). Rechnerischer Festigkeitsnachweis für Maschinenbauteile aus Stahl, Eisenguss- und Aluminiumwerkstoffen. In *Frankfurt am Main: Forschungskuratorium Maschinenbau (FKM)*, vol. 6, (2012)
14. Z. Glavas, A. Strkalj, A. Stojakovic, The properties of silicon alloyed ferritic ductile irons. Metallurgija **55**(3), 293–296 (2016)
15. H. Löblich, W. Stets. *Werkstoff- und fertigungstechnische Grundlagen der Herstellung und Anwendung von hoch siliciumhaltigem Gusseisen mit Kugelgraphit—Teil 1: Einfluss von Silicium auf die mechanischen Eigenschaften, Versprödungseffekte, Seigerungen, Graphitformabweichungen, Wirkung von höheren Gehalten an Mn, Cr und V*. Giesserei, vol. 100, no. 7, pp. 30–47 (2013)
16. P. Weiß, A. Tekavčič, A. Bührig-Polaczek, Mechanistic approach to new design concepts for high silicon ductile iron. Mater. Sci. Eng., A **713**, 67–74 (2018). https://doi.org/10.1016/j.msea.2017.12.012
17. B. Viala, J. Degauque, M. Fagot, M. Baricco, E. Ferrara, F. Fiorillo, Study of the brittle behaviour of annealed Fe-6.5 wt% Si ribbons produced by planar flow casting. Mater. Sci. Eng., A **212**(1), 62–68 (1996)
18. S. Hasse, *Duktiles Gußeisen: Handbuch für Gusserzeuger und Gussverwender*, Edtion edn. (Schiele Schön, Berlin, 1996)
19. G.J. Cox, Entwicklung von besonderen mechanischen Eigenschaften in Gußeisenwerkstoffen mit Kugelgraphit. Giesserei **55**, 127–135 (1968)
20. G.J. Cox, K. Röhrig, Nickel in Gußeisen und Stahlguß. konstruieren + gießen **16**(4), 11–27 (1991)

21. G. Sandoz, H. Bishop, W. Pellini, Notch ductility of nodular irons. Transactions AFS **46**, 418 (1954)

22. M. Hafiz, Mechanical properties of SG-iron with different matrix structure. J. Mater. Sci. **36**(5), 1293–1300 (2001)

23. G. Toktaş, M. Tayanc, A. Toktaş, Effect of matrix structure on the impact properties of an alloyed ductile iron. Mater. Charact. **57**(4), 290–299 (2006)

24. P. Weiß, M. Riebisch, A. Bührig-Polaczek, Mechanical properties and impact toughness of nickel and aluminum alloyed high silicon ductile iron. Mater. Sci. Forum **925**, 304–310 (2018). https://doi.org/10.4028/www.scientific.net/MSF.925.304

25. J. Hernandez-Avila, E. Salinas-Rodriguez, E. Cerecedo-Saenz, I. Rivera-Landero, E. Cardoso-Legorreta, J. Flores-Badillo, M.I. Reyes-Valderrama, The effect of molybdenum on the microstructure of nodular iron. Europ. Sci. J. **11**(36), 337 (2015)

26. S. Hasse, Niedriglegiertes Gusseisen mit Kugelgraphit. Giesserei-Praxis **8**, 293–301 (2005)

27. L.M. Aberg, C. Hartung, Solidification of SiMo nodular cast iron for high temperatur applications. Trans. Indian Inst. Met. **65**(6), 633–636 (2012)

28. S. Obermaier, S. Kleiner, L. Zeipper, M. Kauffmann, SiMo1000—Hochtemperaturbestandiger Gusseisenwerkstoff als Innovation der Georg Fischer Automotive AG. Giesserei-Praxis **7**, 236–242 (2009)

29. Deutsches Institut Für Normung E.V. *DIN 50125: Prüfung metallischer Werkstoffe—Zugproben.* (2000)

30. Deutsches Institut Für Normung E.V. *DIN EN ISO 148-1: Metallische Werkstoffe—Kerbschlagebiegeversuch nach Charpy—Teil 1: Prüfverfahren.* (2016)

31. Internationale Organisation Für Normung. *ISO/FDIS 945-4: Microstructure of cast irons—Part 4: Test method for evaluation nodularity in spheroidal graphite cast irons.* (2019)

32. H. Schumann, H. Oettel, *Metallografie* (Wiley, Hoboken, 2011)

33. M. Riebisch, H.S. Groß, B. Pustal, A. Bührig-Polaczek, Influence of carbide-promoting elements on the pearlite content and the tensile properties of high silicon SSDI ductile iron. Int. J. Metalcast. **12**(1), 106–112 (2018). https://doi.org/10.1007/s40962-017-0146-7

34. M. Riebisch, B. Pustal, A. Bührig-Polaczek, Impact of carbide-promoting elements on the mechanical properties of solid-solutions strengthened ductile iron. Int. J. Metalcast. **14**(2), 365–374 (2020). https://doi.org/10.1007/s40962-019-00358-5

35. S. Vdeh. *Bestimmung der Sprödbruch-Übergangstemperautr FATT und anderer kennzeichnender Größen.* Stahleisen GmbH, (2010)

36. R. T. Titanium. *Ductile Iron Data for Desgin Engineers.* (1998)